Next Generation Technologies for the *in situ* Detection of NO_x Radicals and their Reservoirs from Aircraft and Balloons

Ronald C. Cohen
Department of Chemistry
University of California, Berkeley
Berkeley, CA 94720-1460

***Abstract*- Laser induced fluorescence detection of NO_2 has been developed for application to measurements in the urban and remote atmosphere. Sensitivity better than 1ppt/sec has been demonstrated in the laboratory. The instrument is also combined with thermal dissociation for observation of total peroxynitrates, total alkylnitrates and HNO3. An overview of the instrumentation and some scientific results are described.**

I. INTRODUCTION

The IIP contract NAS1-99053, "Next Generation Technologies for the *in situ* Detection of NO_x Radicals and their Reservoirs from Aircraft and Balloons" was aimed at improving the capabilities of NASA's Earth System Enterprise to validate satellite observations of nitrogen oxides and to understand the processes which govern the global distribution of nitrogen oxides using *in situ* measurements of NO_2, peroxy nitrates, alkyl nitrates and HNO_3. During the course of this 3 year program we made major strides toward development of new technologies for nitrogen oxide detection, including:

- demonstration of a laser-induced fluorescence (LIF) approach to detection of tropospheric NO_2 on the ground and from aircraft, along with demonstration and evaluation of enabling technologies that would improve LIF detection of NO_2 such as alternate spectral features, ultra-high reflectivity mirrors, and calibration sources with high long-term stability
- development and field tests of thermal-dissociation-LIF for observing total peroxy nitrates, total alkyl nitrates and HNO_3
- dramatic improvements to the sensitivity of LIF detection of NO_2 using supersonic expansions, and avalanche photodiodes
- development of a small, simple, and inexpensive LIF system for NO_2 detection based on a commercial cw diode laser

In the following, we briefly review the accomplishments during this project.

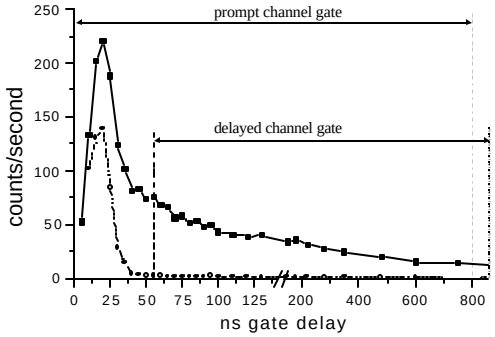

Fig. 1. Timing of NO_2 Signal and N

II. LIF DETECTION OF NO_2

At the outset of this contract we had begun an effort to develop a technique for the observation of NO_2 at concentrations relevant to the remote atmosphere (1-100ppt). IIP support allowed us to finish this development and then to adapt the instrument for use on the NCAR G-130 aircraft. The instrument is described in detail in Thornton et al. [1] Briefly, a compact, diode pumped, Q-switched, frequency doubled, Nd^{3+}: YAG laser (T40-X30, Spectra Physics, average power of 3 watts at 532 nm, 30 ns pulse length) pumps a tunable dye laser at 8 kHz. The home-built, etalon tuned dye laser emits a 25 ns wide (FWHM) pulse with a linewidth of 0.06 cm^{-1} at 585 nm. We tune the laser to excite a narrow rovibronic feature unique to NO_2. The light from the dye laser is focused into a white cell where it makes approximately 40 passes.

Red-shifted fluorescent photons at wavelengths longer than 700 nm are collected and imaged onto the photocathode of a cooled GaAs photomultiplier tube (Hamamatsu H7421-50 or Burle C31034A). The fluorescence signal is directly proportional to the NO_2 mixing ratio. Dichroic filters manufactured using fused silica substrates and without any absorbing components are used to reject Rayleigh, Raman and chamber scatter. Single photons are counted using time-gated photon counting techniques. The detection cells are held at reduced pressure to enable temporal separation of the residual chamber scatter, which is coincident with the laser pulse, and the NO_2 signal which decays exponentially with a pressure dependent time constant (300 ns at 4 torr). Figure 1 illustrates the timing of the

scatter associated with the laser pulse, and the NO_2 flourescence. The separation allows for NO_2 detection with nearly zero background. The laser is alternately tuned between a strong NO_2 resonance and the weaker continuum absorption to test for interferences, assess the background scattering, and for use in an algorithm that holds the laser frequency locked on a single spectral feature. This instrument has detection limit of 10ppt/10sec. The accuracy is 5%, limited primarily by the accuracy of available standards.

We have put significant effort into understanding and streamlining the process of instrument calibration. We measured the quenching rate of NO_2 fluorescence by H_2O, showing that the effect necessitates a correction of approximately 5% at absolute humidity values characteristic of the surface. In the field, we typically calibrate at 150-minute intervals using an NO_2 standard (5.85 ppm in N_2, Scott Specialty Gas) diluted to 1-10 ppb in zero air and compare this to NO_2 standard additions at a similar interval. An example of NO_2 calibration is exhibited in Figure 2. This figure shows the normalized NO_2 counts resulting from flows of various NO_2 mixing ratios that are used together to determine a calibration slope. The reference cylinder is supplied with a low volume pressure regulator that we purge prior to calibration. We also regularly cross-calibrate our NO_2 gas standards of 5, 10, and 50 ppm (Scott Specialty Gases) to verify that the primary standard is not degrading. We have conducted extensive intercomparisons with other NO_2 instruments during the Southern Oxidants Study (SOS, 1999), the Texas Air Quality Study (TEXAQS, 2000), and during the Tropospheric Ozone Production about the Spring Equinox (TOPSE, 2000) campaigns [2].

Modifications to the instrument since the publication of Thornton, et al. [1] include 1) the use of cavity ring down mirrors for the reduction of background scatter, 2) the development of algorithms to perform diagnostics without operator intervention, and 3) optimization of laser output to maximize power over longer time periods. These modifications have improved the signal to noise ratio and have lengthened the time between maintenance to once every 5-7 days.

III. THERMAL-DISSOCIATION COUPLED TO LIF DETECTION OF NO_2

IIP was the sole support for the development and integration of thermal dissociation-LIF (TD-LIF) into a field-tested prototype. The TD-LIF technique is described in detail in a manuscript by Day et al. [3]. The main goal of this work

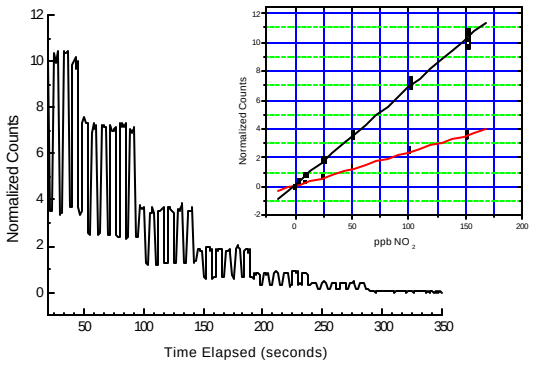

Fig. 2. Typical instrument calibration

was to develop a simple and sensitive technique for the observation of a wide variety of NO_y compounds ($NO_y \equiv HNO_3 + \Sigma R_iONO_2 + \Sigma R_iO_2NO_2 + N_2O_5 + NO_3 + NO_2 + NO$ …). The unique features of TD-LIF include the capability to observe the sum total of different classes of NO_y and to do so with high time resolution. The sampling strategy also provides for high throughput of water soluble species that are notoriously difficult to measure accurately.

Upon heating, most NO_y species thermally dissociate to yield NO_2 and a companion radical:

$$XNO_2 + \text{heat} \rightarrow X + NO_2$$

where X = RO_2, RC(O)OO, RO, OH, HO_2, NO_3, ClO, BrO (1)

Compounds that are detected by NO_y sensors but do not thermally dissociate to produce NO_2 include nitrites (HONO and RONO) and NO_3. N_2O_5 produces 1 NO_2 and 1 NO_3 upon heating. HCN, CH_3CN and NH_3 are known to be interferences to NO_y detectors under some conditions. These compounds do not produce NO_2 upon heating without subsequent chemical reaction. In the TD-LIF instrument, a sample is rapidly heated producing an enhancement in NO_2 over the ambient background. After flowing through a short region that allows the sample to cool to near ambient temperature, the pressure is reduced prior to transport of the radical species to the LIF detection system where NO_2 is observed. The reduced pressure minimizes the potential for interferences from secondary reactions. At a residence time of 30-90ms and a pressure of 1 atm, approximate gas temperatures for complete dissociation are: 200°C for compounds of the form RO_2NO_2 (and N_2O_5); 400°C for compounds of the form $RONO_2$ including both alkyl nitrates and hydroxy nitrates; and finally 650°C for HNO_3. Measured thermal decomposition rates of various compounds within the two organic nitrate classes ($RONO_2$ and $RC(O)O_2NO_2$) exhibit little dependence on what constitutes the 'R'

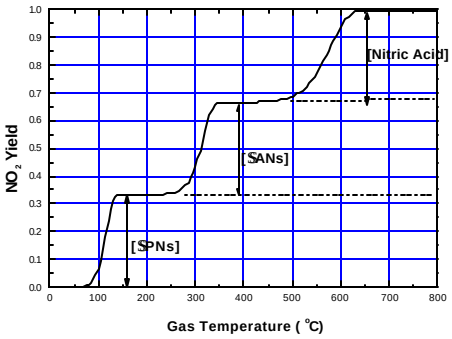

Fig. 3. Theatrical yield of NO_2 from an equal mixture of 3 classes of nitrogen oxides.

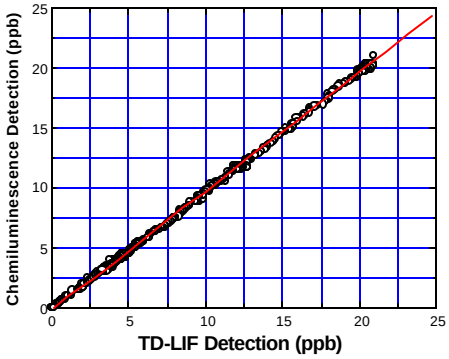

Fig. 4.Comparison of N propylnitrate measured by TD-LIF and Noy

group [4, 5]. The concentration of a class of compounds is determined by the difference between two detectionchannels. For example, HNO_3 is the difference between total NO_2 measured when one inlet heater is set to the nitric acid temperature and a second one is set at the 400°C. The two intermediate classes, total peroxy nitrates and total alkyl nitrates are designated by the shorthand ΣPNs and ΣANs, respectively. If four detection channels (with separate heaters) are employed then the abundances of HNO_3, ΣANs, ΣPNs, and NO_2 can be determined simultaneously. Figure 3 shows a calculation of the NO_2 mixing ratio (above the ambient NO_2) that would be observed as a function of gas temperature if a mixture of equal abundances of ΣPNs, ΣANs, and HNO_3 were sampled.

Laboratory experiments show that TD-LIF works as predicted by theoretical models of the related chemistry. Early engineering problems were primarily associated with materials compatibility and with various seals leaking trace amounts of NO_2 containing compounds into the sample stream upon heating. Several modifications were implemented to address these issues. The heaters were converted to quartz instead of Pyrex, the number of seals was reduced, and temperature cycling of the seals was almost completely eliminated. We also eliminated any residual nitrogen oxide compounds trapped on the surfaces of the instrument by slightly overshooting the target temperature at the beginning of a measurement cycle.

We examined the behavior of a series of nitrogen oxide compounds at different temperatures and compared TD-LIF results to those of a standard commercial NO/NO_y chemiluminescence instrument, and found that the two instruments correlate well. An intercomparison of chemiluminescence detection and TD-LIF of n-propyl nitrate is exhibited in Figure 4. This figure shows a linear fit with slope = 1.01, intercept = -150 ppt, and R^2 = 0.99. Total NO_y measurements by NO/NO_y chemiluminescence have become the standard method for field measurements of nitrogen oxides, so our ability to quantify differences between the two techniques is crucial to our continued work in instrument development. On the basis of the success of the intercomparison between the two techniques, we initiated a long-term comparison of the two different techniques at the UC-Blodgett Forest Research station a site downwind of Sacramento, CA, and located in the Sierra Nevada where we observe a wide range of conditions (high and low humidity, urban plumes, forest fires, dean continental background air, etc.). Analysis of these intercomparisons (in preparation) shows that the two instruments agree, on average, to within 7% during 7 months of atmospheric sampling.

IV. Aircraft Configuration

The NO_2 instrument developed using IIP support was integrated onto the NCAR G130 aircraft during the TOPSE experiment. IIP support was used for integration and instrument evaluation and NSF support for scientific work associated with the project. We integrated a 2-channel instrument with capability for observing NO_2 and ΣPNs by TD-LIF. The instrument was packaged into two bays of a high rack and emphasis on weight reduction and completely eliminating use of 60Hz power simplified operational issues. We also redesigned the thermal dissociation inlet combining elements of an NO_y inlet described by Ryerson, [6] and shorter thermal dissociation ovens (25cm long, 6mm O.D., pyrex tube) that were adequate for ΣPNs, but probably would not work for HNO_3. Intercomparison of our ΣPN measurements with direct measurements made by gas chromatograph-electron capture detection (GC-ECD) of the most abundant peroxy nitrates (PAN and PPN) and with total NO_y chemiluminescence measurements provides evidence of the accuracy of the TD-LIF approach. Figure 5 shows a comparison between all ΣPNs and GC-ECD data taken during TOPSE. A linear fit to the data yields a slope of 0.96 and an intercept of 1.5 pptv, suggesting that the data

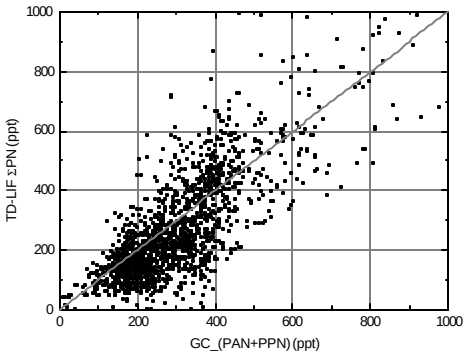

Fig. 5. Comparison of TD-LIF and of peroxy nitrates GC-ECD measurements

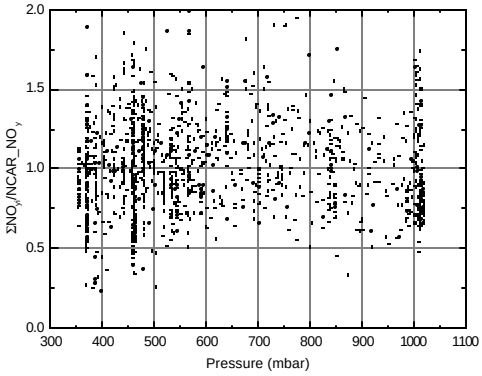

Fig. 6. Ratio of the sum of NO_y compounds measured individually to the total NO_y

agree to within 4% and correlate well (R^2 = 0.77). Evidence also suggested better closure of the NO_y budget using TD-LIF ΣPNs rather than [PAN + PPN] measured by GC-ECD for a range of altitudes. Figure 6 exhibits the sum of individually measured NO_y species (including the TDLIF ΣPNs) divided by NO_y measured by chemiluminescence versus pressure. Substituting the GC-ECD measurements showed a positive trend vs. pressure. The large scatter is indicative of the low mixing ratios and the need for higher precision measurements of many of the NO_y compounds.

V. LIF Detection Of NO_2 Using A Commercial CW Diode Laser

As an alternative to the complex laser system described above and in effort to look forward to the development of simple, powerful diode laser systems, we have optimized the sensitivity of an LIF sensor for NO_2, subject to the design constraint that we utilize a commercially available tunable diode laser. The system is described in detail in a manuscript by Cleary et al. (in preparation for submission to Applied Optics). Of the devices on the market when we began this work, the optimum combination available was determined to be a high resolution (1 MHz) external cavity tunable diode laser (Tui Optics DL-100) at 640 nm, with 16 mW output power. This wavelength has good overlap with the (080) vibronic band in the X^2B_2 state of NO_2. At room temperature strong rotational features in this band have an absorption cross section of approximately 1 x 10^{-20} cm^2.

The cw diode presents different design considerations and options from the pulsed laser system described above. First, since the peak laser power is not very high, there is no concern about saturation of the molecular transition, as is the case for the dye laser. Consequently, we can choose from a range of multi-pass cell geometries and thus minimize chamber scatter. Second, the cw laser does not permit temporal separation of the chamber scatter from the NO_2 fluorescence, making noise reduction more difficult. The laser is focused into a multi-pass Herriot Cell (54 passes) and the fluorescence signal is imaged onto a photomultiplier tube (Hamamatsu H7421-50 Series) mounted perpendicular to the laser beam. The detection cell is a vacuum chamber that includes mounts for spherical Herriot cell mirrors at a separation equal to twice their radius of curvature (4.567 in). We use mirrors with extremely high reflectivity (Research Electro-Optics, Reflectance = 99.998%) because most of the noise in the experiment is due to stray light that results from red-shifted light scatter that is neither transmitted nor reflected by the mirrors. Also, the polarization of the laser is oriented perpendicular to the direction of the detection axis to minimize scattered laser light. In addition to the high reflectivity optics, scattered photons that have their source at (or prior to) the mirrors are minimized by baffles that truncate the solid angle of the mirrors as viewed from the center of the cell. The baffles are arranged as a set of concentric rings and disks forming a cone in space through which the Herriot beams pass. The disks are mounted directly to the Herriot cell mirrors using a hole drilled in the center of each mirror. The rings are mounted in standard 2" optical tubes (THORlabs) The baffles are coated with non-fluorescent flat black spray paint (IIT formula MH2200).

Fluorescence is collected from the center of the cell where the Herriot cell pattern converges to a diameter of 0.6 cm. An 5.08 cm diameter, 6.5 cm focal length plano-convex lens mounted 6.5 cm above the center of the cell collects the fluorescence and produces a nearly collimated beam. An aluminum coated spherical mirror with a 4 cm radius of curvature is mounted 4 cm below the Herriot cell focus. This mirror roughly doubles the photon flux directed at the PMT. The photons then pass through an all dieletric, 740 nm long-pass filter (Omega) which blocks both Rayleigh and some of the Raman resonant laser scatter and most of the red-shifted

scatter light. It is crucial to use filters that are built without absorbing components as these invariably fluoresce adding noise to what is otherwise a nearly zero background experiment. In the prototype described here, we follow this filter with a standard commercial 750 nm long-pass filter (CVI), to block the N_2 and O_2 Raman scattering. Light that passes through the filters is collected by an aluminum coated 5.08 cm diameter, 6.5 cm focal length lens identical to the collection lens and is imaged onto the 5 mm diameter photocathode of the PMT.

The resulting optical system has an approximate geometrical collection efficiency of 1.5×10^{-4} while maintaining a background count rate of 60 counts s^{-1}. Of these, 26 counts s^{-1} are due to the thermal background in the PMT, 10 are due to Raman scattering of 2 counts/Torr/mW (300 mTorr; 16 mW), and 24 are due to laser scatter.

VI. Dramatic Gains In The Sensitivity Of LIF Detection Of NO_2

A. *Supersonic Expansions*

Supersonic expansions are commonly used in the laboratory to produce cold gas phase samples. Low temperatures are advantageous for spectroscopic applications because they reduce spectral congestion by minimizing the number of rotational and vibrational levels that may be populated at room temperature. Consequently, the population and absorption cross-section of low J rotational levels increases.

Jets are produced by gas expansion at high pressure into a vacuum through a small orifice of either circular or linear geometry. Random motion is converted to forward motion during the expansion--the molecules move at high speed in the lab frame of reference but at low speeds relative to one another (and consequently low temperatures). Adiabatic expansion results in cooling of the gas, and collisions maintain equilibrium between the rotational and translational degrees of freedom. Vibrational degrees of freedom also experience cooling but not always as effectively. The cooling achieved is a determined by the number of binary collisions in or near the nozzle which are in turn a function of the pumping speed and gas load. The size of the cold region is also a function of these same parameters, and is given by $l = 0.67d(P_o/P)^{1/2}$ where l is the length of the jet, d the nozzle diameter, P_o the pressure in the nozzle, and P the background pressure in the vacuum chamber. The cold region extends from the nozzle to a Mach disk whose front (at a distance l from the nozzle orifice) acts as a shock wave where collisions of the background gas with the supersonic gas rapidly warms the cooled gas to the chamber temperature. The diameter of the supersonic jet is approximately half the length of the jet.

In our application, we seek to produce a jet that is both cold enough to significantly enhance the NO_2 signal, and long enough to extend through the 6mm diameter laser beam so as to maximize spatial overlap between the jet and the laser beam. These criteria indicate that we require an expansion approximately 2 cm long at a temperature of order 25-50K, conditions which necessitate a chamber pressure in the neighborhood of several hundred millitorr and gas throughput of approximately 8 SLM. Additional constraints include increasing the NO_2 signal without a dramatic increase in the amount of laser scatter. As such, the jet must be long enough that the nozzle does not protrude into the laser beam. Finally, to maintain the portability of our instrument, the supersonic expansion should be accomplished using pumps that are inexpensive, light-weight, and relatively small.

Supersonic jets have been implemented in both the diode and dye laser systems. For both systems, we expand the gas through a 0.3 μm pinhole welded onto the end of a 1/8" diameter stainless steel tube. The pressure in the cell is kept at ~300 mTorr by a small roots blower (an automobile supercharger, Eaton model M-62, 1L/ revolution) with a compression ratio of about 5 backed by a 340 L/min Varian SD-450 mechanical pump. Together, these pumps weigh a modest 100 lbs. This combination of pumping speed and gas load leads to a predicted jet with a 10 mm diameter extending to a Mach disk approximately 14 mm downstream of the pinhole. The predicted rotationally cooling is approximately 25-50 K. Observations of the signal as a function of distance of the nozzle from the laser beam and examination of the relative fluorescence cross-sections of several transitions confirm the accuracy of these calculations.

Experiments using a supersonic expansion at 17094 cm^{-1} in the dye laser system show that the NO_2 signal can be enhanced by nearly a factor of 10 and the signal to noise ratio by $\sqrt{10}$. Figure 7 shows a plot of sensitivity to NO_2 detection (counts per second/ppbv NO_2/laser power) versus pressure expansion ratio in the detection cell. The pressure expansion ratio is the ratio of the pressure on the two sides of the nozzle and is related, as mentioned above, to the jet size and the extent of cooling. We observe that the NO_2 sensitivity depends linearly on the pressure expansion ratio. The current NO_2 sensitivity without cooling is approximately at 0.5 counts s^{-1} mW^{-1} $ppbv^{-1}$ NO_2 (the y-intercept at zero expansion ratio). We expect to be able to increase the pressure expansion ratio and the signal by using a screw compressor supercharger. This type of

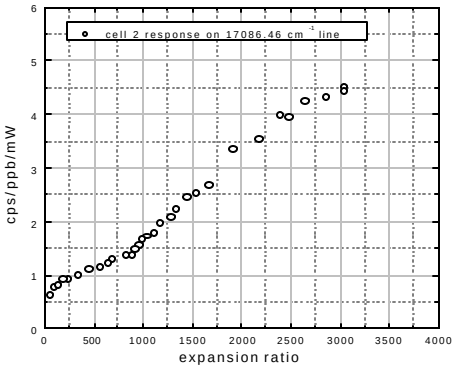

Fig. 7. Sensitivity vs. Expansion Ratio

booster pump has recently been developed for automotive use and has a higher compression ratio than the Roots-type supercharger used for Figure 7 at the same weight.

In the commercial diode laser instrument, we tune the laser to the most intensely fluorescing peak at 15613 cm^{-1} and observe a signal of 14 counts s^{-1} $ppbv^{-1}$ NO_2. Use of the supersonic jet increases the NO_2 fluorescence signal by roughly a factor of 30 over the optimal fluorescing peak at room temperature. In addition, the jet reduces the contribution of the non-resonant fluorescence to a level undetectable above the background noise of the experiment, greatly simplifying the process of assessing whether or not there are interferences. With the background count rate to be 60 counts/s, the overall detection limit is determined to be 150 ppt/ 60s (S/N =2) for this instrument.

B. Avalanche Photodiodes

The GaAs photocathode photomultiplier tubes (PMTs) we use have the highest efficiencies available in the near infrared region (up to 18% in the 700-800 nm range), but become very inefficient at longer wavelengths where much of the NO_2 fluorescence occurs. Silicon avalanche photodiodes (APDs) have the potential for very high quantum efficiencies (80% or more) out to greater than 1100 nm. However, large area APDs have too much dark current (even when cooled to liquid nitrogen temperature) to allow operation at bias voltages greater than breakdown ("Geiger" mode), which is necessary to achieve high gain for every photon absorbed. Instead, the large area APDs must be operated at bias voltages below the breakdown threshold ("gain" mode), and photoelectrons undergo a wide spread of multiplication gains - the most probable of which for a single photon is no gain at all. The gain statistics limit the single photon detection efficiency of a gain mode APD to substantially less than 80%, and imply nonlinearities because two co-incident photons will be detected with more than twice the probability of two photons that arrive at different times.

The large area APDs tested in our laboratory are 8 x 8 mm high gain units manufactured by RMD, Inc. of Watertown, MA. Evaluation on the cw diode laser system revealed nearly three times greater detection efficiency than with the small Hamamatsu PMT. A little than more half of the gain results from the longer wavelength coverage, as estimated from experiments with different filter cut-off wavelengths. The overall signal to noise for the cw system was, however, not improved as the dark count rate from the APD at high gain (>300 counts/sec) was much greater than that of the photomultiplier (<30 counts/sec). For the pulsed laser system with time-gated detection, the gate-on duty cycle reduces effective dark count rate by a factor of 50 or more, depending on the gate width. Further experiments are needed to determine the actual signal to noise gain for the pulsed system, however, we expect a gain of V3 in signal to noise.

VII. SCIENTIFIC RESULTS FROM TD-LIF MEASUREMENTS

The rapid success of our TD-LIF approach allowed us to reach two major scientific conclusions during the course of the IIP contract.

First, the measurements we have made of ΣANs, at Blodgett Forest as part of the evaluation of the TD-LIF method supported by IIP and later in Houston with funding from NOAA and at Granite Bay, CA with funding from DOE-LBNL show unambiguously that ΣANs are the "missing NO_y". For over 15 years most atmospheric field measurements aimed at comparing total nitrogen oxide (NO_y) measurements with the sum of measurements of individual nitrogen oxides have observed a shortfall of individual species. These experiments have let to speculation about the identity of the 'missing NO_y'. Our results from measurements of total alkyl nitrates (ΣANs) from three different field campaigns show that ΣANs are a larger fraction of oxidized nitrogen than has been previously reported. Observations of total NO_y by catalysis followed by chemiluminescence detection and of its components by thermal dissociation-laser induced fluorescence at the U.C. Blodgett Forest Research Station (UC-BFRS) show ΣANs are routinely 10-20% of NO_y with an annual cycle that peaks in late summer. This fractional contribution is nearly an order of magnitude larger than all previous reports of measurements in non-remote regions. Observations at Granite Bay, CA and at LaPorte, TX in summer also show ΣANs to be a large fraction of NO_y in urban centers. Correlations between ΣANs and both peroxy nitrates and ozone show similar behavior to reports of 'missing NO_y'. Taken together

these observations of the fraction of NO_y that is ΣANs, the absolute magnitude of ΣANs, the annual cycle of ΣANs, and correlations with photochemical tracers have led us to conclude that ΣANs are the 'missing NO_y'.

Second, differences between our total ΣPN measurements and the PAN and PPN measurements of Flocke and Weinheimer observed during TOPSE can be associated with the compounds that are expected to be the next most abundant peroxynitrates, HO_2NO_2 and $CH_3O_2NO_2$. The abundances we observe are much less than predicted at cold temperatures (<240K) and are more than predicted at warmer temperatures (240K<T<270K). Detailed analysis of these model measurement discrepancies are described in Murphy et al. [7] confirms the suggestion that near-IR photolysis [8] is a significant contributor to HNO_4 photolysis with a magnitude of 1.5×10^{-5} s^{-1} [9]. The results also suggest that the thermal decomposition rate of $CH_3O_2NO_2$ is faster than in current models (consistent with the only available lab data which current recommendations and models use only as a guide). In models that attempt to represent the atmosphere, these changes in the kinetics will result in a higher abundance of HO_x in the upper troposphere and an increase in the NO_x/NO_y ratio.

VIII. Future Work

Future improvements to the instrumentation developed as part of this IIP contract will likely result from

- engineering to reduce the size and weight, and to improve the reliability of the current instrument
- improved product of laser power and absorption cross-section for the cw diode laser instrument, either with higher power diodes, by coupling to a pulsed diode amplifier, or by using diodes in the blue region of the spectrum
- continued investigation into potential chemical interferences to the TD-LIF instrument
- investigation of the potential for a modified heating strategy to separately identify HO_2NO_2, $CH_3O_2NO_2$ and peroxy acyl nitrates
- extension of TD to detection of nitrite compounds including HONO and RONO.

References

1. Thornton, J.A., P.J. Wooldridge, and R.C. Cohen, Atmospheric NO_2: In situ laser-induced fluorescence detection at parts per trillion mixing ratios. *Analytical Chemistry*, 2000. 72(3): p. 528-539.
2. Thornton, J.T., *Nitrogen Oxide,* Peroxynitrates, and the Chemistry of Tropospheric Ozone Production: New Insights from in situ Measurements, *Ph.D. Thesis, Dept. Chemistry*. 2002, University of California, Berkeley: Berkeley.
3. Day, D.A., *et al.*, A thermal dissociation laser-induced fluorescence instrument for in situ detection of NO_2, peroxy nitrates, alkyl nitrates, and HNO_3. *Journal of Geophysical Research*, 2002. 107(D6): p.
4. Roberts, J.M., The Atmospheric Chemistry of Organic Nitrates. *Atmospheric Environment Part a-General Topics*, 1990. 24(2): p. 243-287.
5. Hao, C.S., *et al.*, Gas Chromatographic Detector For Selective and Sensitive Detection of Atmospheric Organic Nitrates. *Analytical Chemistry*, 1994. 66(21): p. 3737-3743.
6. Ryerson, T.B., *et al.*, Design and initial characterization of an inlet for gas phase NO_y measurements from aircraft. *Journal of Geophysical Research*, 1999. 104(D5): p. 5483-92.
7. .J.G. Murphy, J.A. Thornton, P.J. Wooldridge, D.A. Day, R.S. Rosen, R.C Cohen, C. Cantrell, F. Flocke, B. Lefer, B.A. Ridley, R.E. Shetter, A.J. Weinheimer, R.W. Talbot, Observations of peroxynitrates during TOPSE, submitted to *Geophysical Research Letters* , May 2002.
8. Donaldson, D.J., G.J. Frost, K.H. Rosenlof, A.F. Tuck, and V. Vaida, Atnospheric radical production by excitation of vibrational overtones a absorption of visible light, *Geophysical Research Letters*, 24 (21), 51-2654, 1997.
9. Wennberg, P.O., R.J. Salawitch, D.J. Donaldson, T.F. Hanisco, E.J. Lanzendorf, K.K. Perkins, S.A. Lloyd, V. Vaida, R.S. Gao, E.J. Hintsa, R.C. Cohen, W.H. Swartz, T.L. Kusterer, and D.E. Anderson, Twilight observations suggest unknown sources of HOx, ***Geophysical Research Letters***, 26 (10), 1373-1376, 1999.